Liver Segmentation in Abdominal CT Images by Adaptive 3D Region Growing

Shima Rafiei, Nader Karimi, Behzad Mirmahboub, S.M. Reza Soroushmehr, Banafsheh Felfelian, Shadrokh Samavi, Kayvan Najarian

Abstract—. Automatic liver segmentation plays an important role in computer-aided diagnosis and treatment. Manual segmentation of organs is a difficult and tedious task and so prone to human errors. In this paper, we propose an adaptive 3D region growing with subject-specific conditions. For this aim we use the intensity distribution of most probable voxels in prior map along with location prior. We also incorporate the boundary of target organs to restrict the region growing. In order to obtain strong edges and high contrast, we propose an effective contrast enhancement algorithm to facilitate more accurate segmentation. In this paper, 92.56% Dice score is achieved. We compare our method with the method of hard thresholding on Deeds prior map and also with the majority voting on Deeds registration with 13 organs.

I. Introduction

Liver, the largest abdominal organ is in the risk of trauma, chronic diseases and ongoing cancers. In the United states the number of people with liver cancer has been tripled since 1980 and the general 5-year survival rate is 18% [1]. Nevertheless, diagnosing of this vital organ at early stages would increase the rate of survival and recovery. In this regard, computed tomography (CT) scans are analyzed by radiologist for pre-diagnosis, treatment and staging. Every day radiologists spend a lot of time for analysis of organs within CT scans. However, computer-aided diagnosis (CAD) such as automatic liver segmentation can accelerate the process of scan analysis.

Knowing the exact shape, size and location of an organ help physicians to better understand about diseases and decide how to do surgeries. This is a challenging task because of different shapes of organs between patients due to disease or various body anatomies. Inter-patient variability such as organ shape, size and also appearance makes the necessity for organ localization in the form of bounding boxes or location prior map before any step of segmentation. Generally, the organ detection and segmentation can be categorized into three different kinds of methods i.e. imagebased, atlas-based and learning-based. The first one is

application-specific and does not evaluate different image condition. Jang et al. [2] applied a region growing approach for segmenting the lungs to help localizing the liver. Atlasbased approaches look for spatial relationship and shape among atlas data and are relatively useful for those with high variability. However, these methods are computationally expensive due to registration steps. Xu et al. [3] evaluated six famous registration methods for human abdominal organs on 1000 CT scans. Consequently, the Deeds method was introduced as the most efficient and accurate registration method for abdominal organs. After applying registration approach, prior models can be deduced from labels of transformed atlases. These priors capture location and shape information that exist between slices. For this aim, probabilistic atlas [4],[5] along with shape-prior, such as statistical shape model [6],[7], are applied to exploit prior knowledge of atlas data for more robust organ segmentation. On the other hand, learning-based approaches for organ localization such as decision forest [8] and regression forest [9] localize several organs without any registration. Even though these methods have efficient computation time, they are not efficient for organs with large variations in shape and location.

In this paper, we combine location priors achieved by Deeds registration method and 3D adaptive region growing. We first estimate a probability location map using all registered atlases. After preprocessing step that improves image quality by strengthening its edges and contrast, we obtain boundary mask of abdomen slices. The boundary mask along with prior location map help region growing algorithm to be restricted to a relatively appropriate ROI. In this method we apply adaptive region growing with dynamic condition of intensity. Since the organ intensity can vary among patients, hard thresholding for intensity condition cannot be effective without supervised intensity information. Due to this fact we calculate the mean and variance of intensity among the most probable voxels of a target organ and adjust the intensity condition based on these subjectspecific parameters. The remaining of this paper is organized as follow. In Section II we describe our proposed method including the description of calculating location prior map, our preprocessing method and the proposed image-based segmentation approach. In Section III, we evaluate our method on 30 CT scans to segment liver organs and show the experimental results qualitatively. Finally, Section IV concludes the paper and we mention the superiorities and shortcomings of the proposed method.

S. Rafiei, N. Karimi, and S. Samavi are with the Department of Electrical and Computer Engineering, Isfahan University of Technology, Isfahan 84156-83111, Iran.

B. Mirmahboub is a member of Pattern Analysis and Computer Vision (PAVIS) department in Italian Institute of Technology, Italy.

S.M. R. Soroushmehr and K. Najarian are with the Department of Computational Medicine and Bioinformatics and Michigan Center for Integrative Research in Critical Care, University of Michigan, Ann Arbor, MI. U.S.A.

B. Felfeliyan is a research assistant at the Foothills Hospital, University of Calgary, Canada.

II. PROPOSED METHOD

A. Deeds registration

Since an abdominal organ has large variety of shape and location from patient to patient, organ segmentation without involving location information can encounter with major errors. Due to this fact, we need to detect an ROI containing liver voxels with large sensitivity to assign correct labels in the segmentation level. Hence in this paper, the organ localization in the form of location prior map is estimated using atlas scans annotated by experts. Fig. 1 shows the overview of our proposed method. Since the size and direction of bodies are different among atlas patients, the affine transformation [10] method is applied to make source scans, or atlases, with the same size and direction of the target scan, or the test patient. After the affine transformation, non-rigid deformation with Deeds method [10] is applied to deform the content of atlas scan to reach a relatively similar content of target. This deformation is done with Deeds method that is Markov Random Field (MRF)based [11] and uses self-similarity context [12] as a discriminative descriptor that is independent of intensity. Indeed it discriminates corner points from homogenous intensities and gradients of boundary in multi-modal medical images [13]. Hence we registered raw sources with each target, with no necessity for image enhancement. However, all registration methods suffer from sticking in local optima and in some cases result in dissatisfied deformation. To mitigate this issue, we introduce a probability map that incorporates multi-atlas location prior and approximate location of liver in target patients.

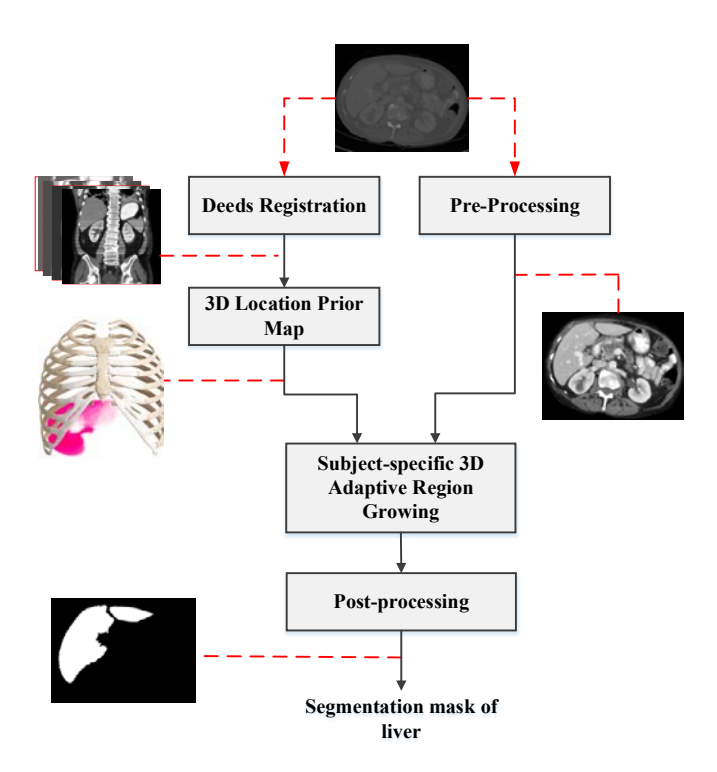


Fig.1. block diagram of the proposed method.

B. 3D Probability location map

For each patient a separate probability map is calculated as in Eq. 1. Assume that we have one target patient and M-1 registered sources with N axial slices for each one. Then $S_{i,j}$ denotes a binary mask of j^{th} slice of registered label in the i^{th} source. Each pixel in binary mask is labeled as 1 and 0 to denote "liver" and "non-liver" respectively. The probability map for target patient relative to sources can be simply estimated as sum of all source scans. Therefore, if a single voxel has liver label in many source scans, it will be assigned more probability value rather a voxel that has non-liver label in most of the source scans. The above explanation can be formulated as (1) where P_j is j^{th} axial slice of the probability map and M is the whole number of available scans containing target scan. M-1 used for normalization, attaining probability map.

$$P_{j} = \frac{1}{|M-1|} \sum_{i=1}^{M-1} S_{i,j} , \quad j \in \{1, ..., N\}$$
 (1)

However, source scans are very different from each other and some of them might mislead the probability map that affects the final decision of target labels. To mitigate this issue, along with this prior map we involve each slice context in a scan to improve the final result. For this goal, to achieve more powerful intensity or edge context, we first propose a preprocessing approach appropriate for abdominal scans.

B. Preprocessing

Medical images usually lack sharp and accurate boundaries. The segmentation algorithm has to struggle with vague borders with low contrast. As for abdominal CT scans, joint borders among organs tissues, CT artifacts and noises in addition to similar intensity of neighboring viscera are the most essential issues. Hence, to mitigate this issue, we apply a preprocessing algorithm on abdominal scans which improves the following image-based segmentation algorithm. The raw scan has a long range of -1000 to +3000 HU from the air that exists in lungs to spline bones. On the other hand, range of HU differs in organs tissue from +100 to +300 which is relatively short range with low contrast. For stretching the contrast of liver and its neighboring tissues, we design a four-step preprocessing algorithm. First, the ROI of abdominal area in each slice of a person is extracted using Otsu thresholding method. Using this threshold, all organs tissue with positive HU are selected while the air voxels with negative HU are eliminated. Then we vectorize all pixels in the abdominal ROI of all slices and normalize their intensities within 0 to 255. An enhanced scan is constructed using these adjusted intensities. In final step a guided filter [14] is applied to the image to reduce noise. Guided filter is an edge-preserving smoothing operator which generates output filtered image, considering the content of a guidance image. Consequently, by creating high contrast, this stage turns the weak borders into relatively strong boundaries. Fig.2. illustrates the enhanced scan after extracting interested region in each slice of a scan.

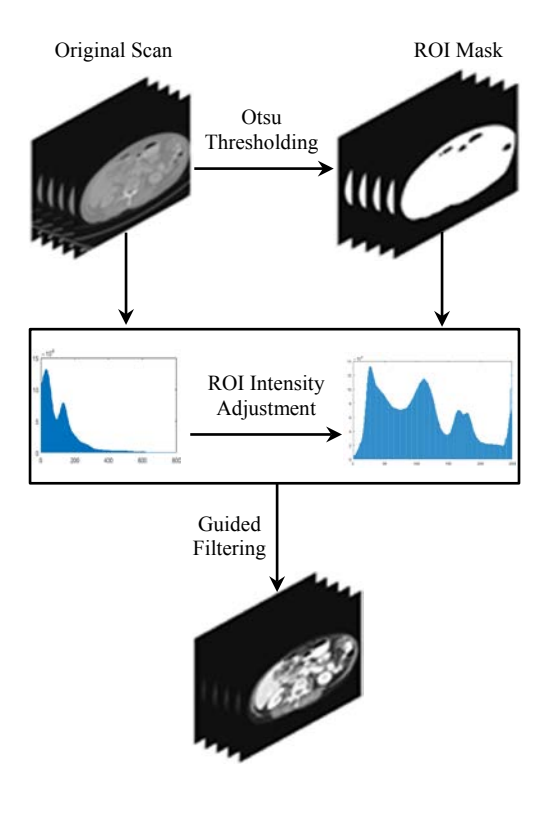


Fig.2. Preprocessing algorithm to enhance image contrast.

In previous section, we attained a prior map that contains approximate shape, location and surface priors for liver which needs to be enhanced by a segmentation algorithm. Here we employ region growing algorithm [15] to precisely segment the liver. Region growing algorithm starts from initial region and iteratively grow the region by comparing all unallocated neighboring pixels. This algorithm considers each voxel's neighborhood in 3D view (i.e. 26 voxels around it). By using the neighborhood information that exist in probability map, the segmentation will be more robust to the noise.

We set some conditions for a voxel with the index of $V = (v_x, v_y, v_z)$ to join the region. The first condition for region growing is not selecting voxels on boundary. This condition restricts the grown region inside the organ boundary. Although many small boundaries exist inside the organ, our algorithm ignore them in this stage. The second condition considers intensity constraint besides location prior. First, If the neighborhood of V, on the average, consists of voxels with higher probability than a threshold T_2 , this voxel will join the region during growing without any constraint on its intensity. This condition is commonly triggered when the voxel is located inside the liver tissue. This voxel is confident due to high confidence of its neighbor voxels even if it has dissimilarity in its own intensity. In this situation some very light or dark spots that are located on liver tissue cannot make trouble for the algorithm. The second sub-condition adds a voxel that its intensity is near to the most probable voxels. We consider the most probable initial regions, Q, where voxels have 70 percent confidence or more according to prior map and calculate the mean and variance of their intensities. A new voxel is added to the region if its average intensity is near the average intensity of most probable voxels and not farther than k times of their variance. Even though this condition is very effective thanks to the proposed preprocessing step, it is not sufficient in some slices with weak contrast. For example, a large number of voxels around liver tissue have similar intensity except dark voxels that are related to the air in lung and gastrointestinal organs. To address this issue, we consider the threshold T_1 on the voxel location prior probability. If the $m \times m$ neighborhood of V on the average consists of voxels with higher probability than T_1 , the center voxel V is added into the growing region. Briefly, a voxel V is added to the region

(1) *V* \notin *Organ Boundary*

$$(2) \begin{cases} A \geq T_2 & where \ A = \frac{1}{N} \sum_{i=-m}^{m} \sum_{j=-m}^{m} P(v_x + i, v_y + j, v_z) \\ or \\ A \geq T_1 & and \quad |I(V) - mean(Q)| \leq k \times variance(Q) \end{cases}$$

where A is the average probability of surrounding voxels, I(V) is the intensity of the voxel V and Q is the set of most probable voxels that is defined in the prior location map.

These conditions would restrict the region growing algorithm in a predefined ROI, where the region cannot grow beyond that ROI. Even if the boundary in some part of the organ have been vanished, the prior location will stop growing to exceed the boundary. In addition, instead of hard threshold for intensity, the intensity constraint makes the intensity condition specific for the target. Finally, the algorithm stops when no voxel found satisfying the conditions.

C. Post processing

The binary mask achieved by region growing is processed by morphological operations for boundary enhancement and filling the internal holes.

III. EXPERIMENTAL RESULTS

A. Database

Our dataset is publicly available ontaining 30 patients with total of 3631 CT slices. This dataset was provided Under Institutional Review Board (IRB) that were selected among patients with ongoing colorectal cancer or retrospective ventral hernia. The dataset volume sizes are $(512 \times 512 \times 85) \sim (512 \times 512 \times 198)$ while all scans were in portal-venous contrast phase. These scans were captured with various field of views of $(280 \times 280 \times 280) \sim (500 \times 500 \times 650)$ mm3 and resolution of $(0.54 \times 0.54 \times 5.0) \sim (0.98 \times 0.98 \times 2.5)$ mm3.

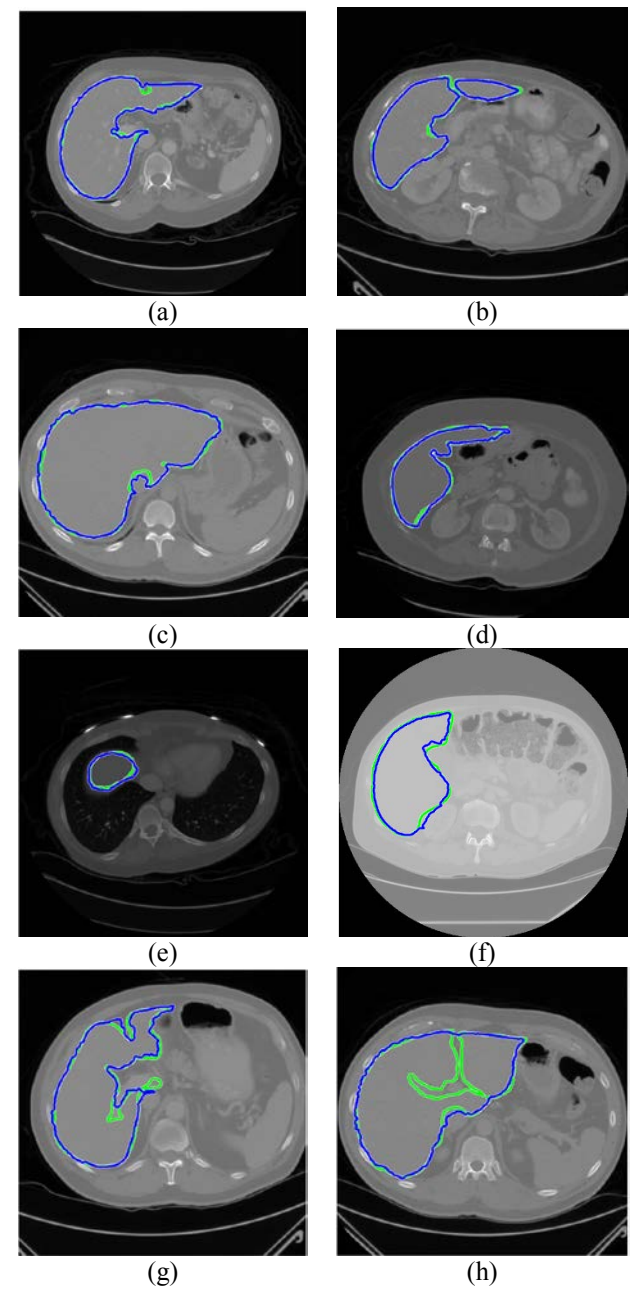


Fig. 3. Segmentation results of proposed method on axial slices containing liver. Ground-truths boundaries shown in green. Results of the proposed method shown in blue. (a-f) perfect segmentations, (g-h) mistakes of the algorithm due to extraordinary shapes of liver.

In this paper, Deeds registration parameters are set similar to [3]. The parameters used in region growing such as threshold T_1 have been set as 0.1 while the threshold T_2 have been set as 0.7 probability. The k is set to 2 while m is 3, constructing 3×3 2-dimensional neighborhood.

In this paper, we applied our proposed method on 30 CT scans and achieved 92.56% Dice score on the average. In Table 1 our comparison is with Deeds registration method, where a simple hard thresholding of 50 percent is used on the liver organ. Another comparison is also on Majority voting of 13 organs labels, e.g. spleen, kidneys, gallbladder,

esophagus, liver, stomach, aorta, inferior vena cava, portal vein and splenic vein, pancreas, right and left adrenal gland.

Fig.3 illustrates the final results. The boundary of segmentation mask is overlaid on original slices of different scans. The blue boundary depicts the proposed segmentation while the green one is ground truth. In Fig. 3(a-f) the proposed method obtained appropriate segmentation results successfully; however, cases shown in Fig. 3(g-h) are relatively challenging. In Fig. 3(e) the scan contrast is changed abruptly while reaching the upper slices near the lung. In Fig. 3(f) the scan seems to be captured with different condition since an opaque circle appears around the whole body scan. This circle is eliminated in preprocessing stage and the scan attain normal contrast. Fig. 3(g-h) illustrate main issues of this proposed method i.e. jagged borders and filling holes inside the liver.

Table 1. Comparison with Deeds approaches of liver segmentation applied to the MICCAI 2015 abdominal database scans. Best results are bolded.

	Segmentation performance		
Segmentation algorithms	Dice Score (%)	Sensitivity (%)	Jaccard (%)
Deeds hard- thresholding	56.32	99.74	39.79
Deeds majority voting	89.78	89.32	82.08
Proposed method	92.56	93.42	86.29

IV. CONCLUSION

In this paper, we utilized Deeds registration method to produce 3D location prior map of the liver organ. After a preprocessing stage that enhances the contrast, we designed an adaptive 3D region growing based on intensity, boundary and location constraints. We also considered the location constraint in an $m \times m$ neighborhood that significantly improved the results of region growing and made our image-based segmentation method more stable. Experimental results showed that most of the errors happened on boundaries especially where the boundary constraint could not stop growing due to weak and unclear borders between organs.

REFERENCES

- [1] "Liver Cancer: Statistics." 09-Jan-2012.
- [2] Y. Jang, H. Hong, J. W. Chung, and Y. H. Yoon, "Automatic segmentation of the liver using multi-planar anatomy and deformable surface model in abdominal contrast-enhanced CT images," 2012, vol. 8314, no., pp. 831436–831438.
- [3] Z. Xu *et al.*, "Evaluation of six registration methods for the human abdomen on clinically acquired CT," *IEEE Trans. Biomed. Eng.*, vol. 63, no. 8, pp. 1563–1572, 2016.
- [4] H. Park, P. H. Bland, and C. R. Meyer, "Construction of an abdominal probabilistic atlas and its application in segmentation," *IEEE Trans. Med. Imaging*, vol. 22, no. 4, pp. 483–492, 2003.
- [5] N. Farzaneh et al., "Liver Segmentation Using Location and Intensity Probabilistic Atlases *," pp. 6453–6456, 2016.
- [6] T. Heimann and H. P. Meinzer, "Statistical shape models for 3D medical image segmentation: A review," *Med. Image Anal.*, vol. 13, no. 4, pp. 543–563, 2009.

- [7] T. Okada, M. G. Linguraru, M. Hori, R. M. Summers, N. Tomiyama, and Y. Sato, "Abdominal multi-organ segmentation from CT images using conditional shape-location and unsupervised intensity priors.," *Med. Image Anal.*, vol. 26, no. 1, pp. 1–18, Dec. 2015.
- [8] A. Criminisi, J. Shotton, and S. Bucciarelli, "Decision forests with long-range spatial context for organ localization in CT volumes," MICCAI Work. Probabilistic Model. Med. Image Anal., pp. 69– 80, 2009.
- [9] A. Criminisi et al., "Regression forests for efficient anatomy detection and localization in computed tomography scans," Med. Image Anal., vol. 17, no. 8, pp. 1293–1303, 2013.
- [10] mattiaspaul, "deedsBCV: new and more efficient version for 3D discrete deformable registration, reaching the highest accuracy in several benchmarks," 16-Nov-2017. [Online]. Available: https://github.com/mattiaspaul/deedsBCV.
- [11] M. P. Heinrich, M. Jenkinson, M. Brady, and J. A. Schnabel, "MRF-Based deformable registration and ventilation estimation

- of lung CT," *IEEE Trans. Med. Imaging*, vol. 32, no. 7, pp. 1239–1248, 2013.
- [12] M. P. Heinrich, M. Jenkinson, B. W. Papiez, S. M. Brady, and J. A. Schnabel, "Towards realtime multimodal fusion for image-guided interventions using self-similarities.," *Med. Image Comput. Comput. Assist. Interv.*, vol. 16, no. Pt 1, pp. 187–94, 2013
- [13] M. P. Heinrich et al., "MIND: Modality independent neighbourhood descriptor for multi-modal deformable registration," Med. Image Anal., vol. 16, no. 7, pp. 1423–1435, 2012.
- [14] K. He, J. Sun, and X. Tang, "Guided image filtering," IEEE Trans. Pattern Anal. Mach. Intell., vol. 35, no. 6, pp. 1397–1409, 2013
- [15] R. Pohle and K. D. Toennies, "Segmentation of Medical Images Using Adaptive region Growing," in *SPIE 4322, Medical Imaging 2001.*, 2001, pp. 1337–1346.